Optica Applicata, Vol. XLVIII, No. 1, 2018
DOI: 10.5277/oa180105

Defect modes properties in one-dimensional photonic crystals employing a superconducting nanocomposite material

ARAFA H. ALY*, HUSSEIN A. ELSAYED, CHRISTINA MALEK

Physics Department, Faculty of Science, Beni-Suef University, Egypt

*Corresponding author: arafa.hussien@science.bsu.edu.eg

In the present work, we investigate theoretically the transmission characteristics of one-dimensional photonic crystals that contain a defect layer of a nanocomposite material in infrared radiation. The theoretical treatment is obtained depending on the fundamentals of the characteristic matrix method. Here, the nanocomposite designed from nanoparticles of a superconducting material is arranged into a dielectric medium. The numerical results clarify the acute effect of the volume fraction and the operating temperature on the effective permittivity of the nanocomposite material. Therefore, the volume fraction, the operating temperature and other parameters such as the permittivity of the dielectric material and the threshold frequency could have a significant effect on the characteristics of the defect modes. Thus, our structure may be very promising in many applications such as narrow band filters and among optoelectronic applications.

Keywords: photonic crystals, band gap, defect mode, nanocomposite.

1. Introduction

In recent time, photonic crystals (PCs) received considerable attention in the field of optical applications due to their peculiar characteristics. PCs derived their properties from the periodic modulation of the refractive indices of the constituent materials in one, two, and three-dimensions [1–5]. Therefore, PCs have a noticeable effect on the controlling of the electromagnetic waves propagation due to the appearance of the photonic band gaps (PBGs) [6, 7], and photon localization [8, 9]. PBGs present the ability of the full control of the propagation of electromagnetic waves of certain frequencies due to the interference of the Bragg scattering [10].

On the other hand, photon localization grants PCs another advantage by the appearance of discontinuous electromagnetic frequencies in the PBG. These intermittent electromagnetic frequencies appear due to the broken periodicity of the structure that can be obtained by changing the thickness of materials, or by adding or removing a layer of the structure [11, 12]. Therefore, the interference behavior of the incident waves

through the structure could be changed owing to the presence of this disorder within the structure.

These unusual properties make PCs the cornerstone of several applications such as optical filters [13–15], optical fibers [16] and optical switches [17, 18].

Moreover, the inclusion of the dispersive materials on the design and the fabrication of many devices that are particularly depending on PCs received a considerable attention owing to the novel properties of such materials [19–22]. For example, metals possess high reflectivity, therefore they may have a significant effect on PCs over other types of materials such as dielectrics and semiconductors [19]. However, the high values of absorption at large thicknesses of the metallic layer impose some restrictions on the usage of metals in PCs applications [11].

The considerable attention is devoted towards the inclusion of superconductors in PCs depending on their novel properties [13, 20, 23]. Moreover, the addition of nanocomposite materials in PCs has many useful features such as the appearance of new PBGs and the high sensitivity to the polarization modes reliance on the high optical dispersion in the region of plasmon resonance of such materials [24–29].

In this paper, we intend to investigate the transmittance characteristics of 1D PCs that contain a defect layer of a nanocomposite material. Here, the nanocomposite material is composed of a superconducting material (Nb) surrounded by a dielectric material of MgF_2. The theoretical analysis is based on the well-known characteristic matrix method, while the defect layer is homogenized through a standard Maxwell–Garnett procedure. Furthermore, we demonstrate the ability to control the position and the intensity of the localized mode depending on many parameters such as the nanocomposite layer permittivity, the operating temperature of the superconducting material, the refractive index of the dielectric material and the volume fraction.

2. Theoretical analysis

In this section, we have investigated the theoretical model that describes the interaction of the incident electromagnetic waves with our structure [30]. Here, we use two dielectric media A and B of thicknesses (d_1 and d_2) and refractive indices (n_1 and n_2), re-

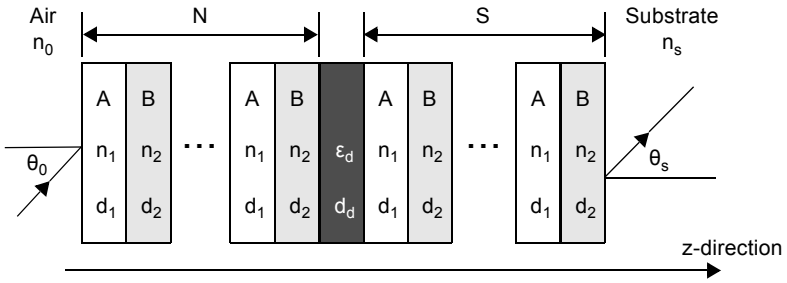

Fig. 1. Schematic diagram of 1D PCs that contains a defect layer. Here, the thicknesses of the dielectric media are denoted by d_1 and d_2, respectively, and that of defect layer is d_d. The corresponding refractive indices are separately indicated by n_0, n_1, n_2, n_d, and n_s, where n_0 is taken for air and n_s is for the substrate.

spectively, to design the periodic structure. The defect layer is sandwiched between two identical periodic structures that are repeated for N and S periods, respectively. Then, the whole structure is immersed in air and substrate as shown in Fig. 1.

Based on the fundamentals of the characteristic matrix method, the interaction between the incident electromagnetic waves and our structure can be described by the following matrix:

$$M = \begin{pmatrix} M_{11} & M_{12} \\ M_{21} & M_{22} \end{pmatrix} = Q(Na)D(d_{\mathrm{d}})W(Sa)$$

$$= \begin{pmatrix} Q_{11} & Q_{12} \\ Q_{21} & Q_{22} \end{pmatrix} \begin{pmatrix} d_{11} & d_{12} \\ d_{21} & d_{22} \end{pmatrix} \begin{pmatrix} W_{11} & W_{12} \\ W_{21} & W_{22} \end{pmatrix} \tag{1}$$

The first and the third matrices are used to describe the left and the right periodic structures, respectively. Wherein, the second one represents the defect layer. Then, the matrix that represents the left periodic structure is given by

$$Q(a) = \begin{pmatrix} q_{11} & q_{12} \\ q_{21} & q_{22} \end{pmatrix}$$

$$= \begin{pmatrix} \cos(\alpha_1) & -\dfrac{i}{\delta_1}\sin(\alpha_1) \\ -i\delta_1 \sin(\alpha_1) & \cos(\alpha_1) \end{pmatrix} \begin{pmatrix} \cos(\alpha_2) & -\dfrac{i}{\delta_2}\sin(\alpha_2) \\ -i\delta_2 \sin(\alpha_2) & \cos(\alpha_2) \end{pmatrix} \tag{2}$$

Since $a = (d_1 + d_2)$ and a is the lattice constant.

$$\alpha_i = \frac{2\pi d_i}{\lambda} n_i \cos(\theta_i), \quad i = 1, 2 \tag{3}$$

and

$$\delta_i = n_i \cos(\theta_i), \quad i = 1, 2 \tag{4}$$

where $Q(Na)$ is the matrix for N period, and Q_{11}, Q_{12}, Q_{21} and Q_{22} are parts of their elements that can be related to the elements of the single period matrix (q_{11}, q_{12}, q_{21} and q_{22}) by

$$Q(Na) = \begin{pmatrix} Q_{11} & Q_{12} \\ Q_{21} & Q_{22} \end{pmatrix}$$

$$= \begin{pmatrix} q_{11}U_{N-1}(\varphi) - U_{N-2}(\varphi) & q_{12}U_{N-1}(\varphi) \\ q_{21}U_{N-1}(\varphi) & q_{22}U_{N-1}(\varphi) - U_{N-2}(\varphi) \end{pmatrix} \tag{5}$$

where

$$\varphi = 0.5(q_{11} + q_{22}) \tag{6a}$$

$$U_N(\varphi) = \frac{\sin\left[(N+1)\cos^{-1}(\varphi)\right]}{\sqrt{1-\varphi^2}} \tag{6b}$$

In addition, the matrix that describes the right periodic structure is the same as for the left periodic structure. For the nanocomposite material, the nanoparticles are randomly distributed in a transparent matrix. Therefore, the permittivity of the nanocomposite ε_{eff} can be described by Maxwell–Garnett formula as

$$\varepsilon_{\text{eff}} = \frac{2\varepsilon_{\text{m}}\eta(\varepsilon_{\text{p}} - \varepsilon_{\text{m}}) + \varepsilon_{\text{m}}(\varepsilon_{\text{p}} + 2\varepsilon_{\text{m}})}{2\varepsilon_{\text{m}} + \varepsilon_{\text{p}} + \eta(\varepsilon_{\text{m}} - \varepsilon_{\text{p}})} \tag{7}$$

where ε_{m} is the permittivity of dielectric material, ε_{p} is the permittivity of superconductor nanoparticles, and η is a volume fraction of the nanoparticles. The permittivity of the superconductor material is frequency dependent, which can be described based on the conventional two fluid models [30]. Thus, the electromagnetic response of a superconductor can be described in terms of the complex conductivity $\sigma = \sigma_1 - i\sigma_2$ where σ_1 and σ_2 indicate the losses contributed by the normal electrons and the super-electrons, respectively. The imaginary part is expressed as [31]

$$\sigma_2 = \frac{1}{\omega\mu_0\lambda_{\text{L}}^2} \tag{8}$$

where λ_{L} is the temperature dependent London penetration depth that is given as

$$\lambda_{\text{L}} = \lambda_{\text{L}}(T) = \frac{\lambda_0}{\sqrt{1-(T/T_{\text{c}})^4}} \tag{9}$$

and λ_0 is the penetration depth at $T = 0$ K, T is the operating temperature, and T_{c} is the transition temperature of the superconductor.

At the critical temperature T_{c} the superconducting phase vanishes, while as $T \to 0$, the contribution of the normal electrons is negligible and the conductivity reduces to

$$\sigma = -i\sigma_2 = \frac{-i}{\omega\mu_0\lambda_{\text{L}}^2} \tag{10}$$

Therefore, the dielectric constant can be described as

$$\varepsilon_{\text{p}} = 1 - \frac{c^2}{\omega^2\lambda_{\text{L}}^2} = 1 - \frac{\omega_{\text{th}}^2}{\omega^2} \tag{11}$$

where ω_{th} is the threshold frequency of the superconductor material and c is the velocity of light in vacuum. Then, the matrix that describes the defect layer can be written as

$$D_d = \begin{pmatrix} d_{11} & d_{12} \\ d_{21} & d_{22} \end{pmatrix} = \begin{pmatrix} \cos(\alpha_d) & -\frac{i}{\delta_d}\sin(\alpha_d) \\ -i\delta_d \sin(\alpha_d) & \cos(\alpha_d) \end{pmatrix} \tag{12}$$

Then, the whole matrix enables us to calculate the transmission coefficient t from the following relation:

$$t = \frac{2p_0}{(M_{11} + M_{12}p_s)p_0 + (M_{21} + M_{22}p_s)} \tag{13}$$

where

$$p_0 = \sqrt{\frac{\varepsilon_0}{\mu_0}}\, n_0 \cos(\theta_0) \quad \text{and} \quad p_s = \sqrt{\frac{\varepsilon_0}{\mu_0}}\, n_s \cos(\theta_s) \tag{14}$$

Finally, we can calculate the transmittance by using the following expression

$$T = \frac{p_s}{p_0}\left|t^2\right| \tag{15}$$

3. Results and discussions

Here, we present the numerical results of the electromagnetic waves propagation through 1D PCs that contain a defect layer of a nanocomposite material in IR region. We use two different dielectric materials to design our periodic structure, *i.e.*, the first material is Si with refractive index $n_1 = 3.3$ and thickness $d_1 = 90$ nm, wherein, the second material is SiO_2 with refractive index $n_2 = 1.4618$ and thickness $d_2 = 200$ nm. Then, the defect layer is a nanocomposite material that contains nanoparticles of Nb superconductor embedded into a dielectric medium of MgF_2. The superconducting material is characterized by $T_c = 9.2$ K, $\lambda_0 = 83.4$ nm [20] and operating temperature $T = 4.2$ K. Moreover, the thickness of the defect layer is set to be $d_d = 120$ nm. The refractive index of the substrate is taken to be $n_s = 1.5207$. Wherein, the number of periods are $N = S = 5$. We present our results in three stages. First, we discuss the dependence of the nanocomposite material permittivity on the volume fraction and the operating temperature of the superconducting nanoparticles. Second, we investigate the transmission characteristics of 1D PCs in the presence of the nanocomposite material as a defect layer. Finally, we demonstrate the effect of some parameters on the transmission properties of our structure such as the volume fraction, the operating temperature, the permittivity of the nanoparticles and the permittivity of the dielectric material. Figure 2 indicated the effect of the volume fraction and the operating temperature on the permittivity of the nanocomposite material. Figure 2**a** shows the dependence of the nanocomposite material permittivity on the volume fraction. The figure shows a significant effect of the

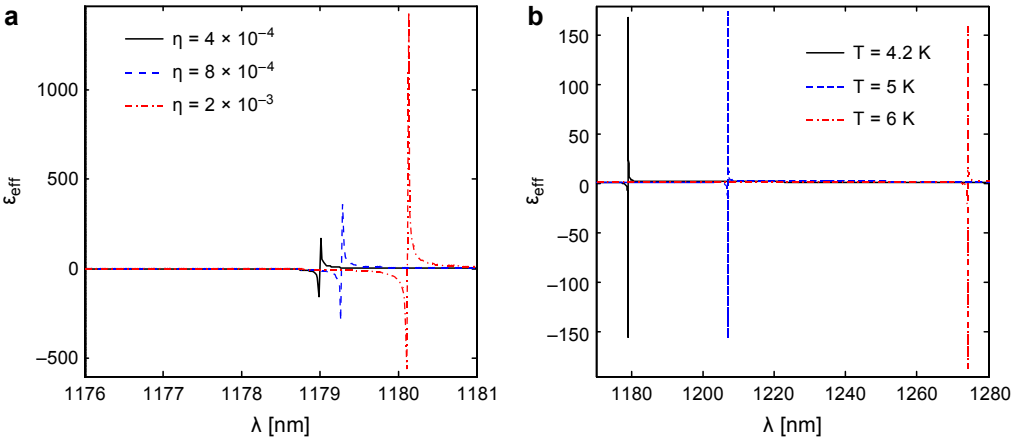

Fig. 2. The variation of the effective permittivity of the nanocomposite material with the wavelength at different volume fraction (**a**) and different operating temperature (**b**).

volume fraction on the permittivity. Besides, there is a resonance peak which appears at the wavelength greater than 1179 nm. This peak is obtained at the resonance wavelength of the nanocomposite materials. Here, the peak intensity is strongly affected by the value of the volume fraction. However, the position of this resonance peak is slightly modified with the increments of the volume fraction. Also, the permittivity of the nanocomposite material decreases the negative values downwards by the increase of the volume fraction at wavelengths smaller than the wavelength of the resonance peak. Then, it begins to grow towards the positive values with the volume fraction increment at wavelengths greater than the wavelength of the resonance peak. On the other hand, Fig. 2**b** describes the dependence of the nanocomposite material permittivity on the operating temperature of the nanoparticle at $\eta = 4 \times 10^{-4}$. The figure shows that the values of permittivity are almost unaffected by the operating temperature. However, the resonance peak shifted towards higher wavelengths values with the increase of the operating temperature

In the second stage, we investigate the transmission characteristics of 1D PCs in the presence of the nanocomposite as a defect layer. Here, the volume fraction is taken to be $\eta = 4 \times 10^{-4}$. Figure 3 shows the variations of the transmittance values *versus* the wavelength of the incident radiation for both periodic and defective 1D PCs in the case of normal incidence. In the case of periodic 1D PCs, a wide PBG is observed in IR regions with bandwidth of 639 nm. Wherein, the band edges of this gap are located at 939 and 1178 nm, respectively. In the presence of the defect layer of a nanocomposite material, the width of the PBG increased to reach 701 nm. Furthermore, the inclusion of the defect layer leads to the appearance of two narrow peaks that are located at 1041 and 1179 nm, respectively, as shown in the figure. Here, the intensity of the first defect mode reaches to more than 0.98, wherein the intensity of the second peak is about 0.24. The peak appears due to the broken periodicity of the structure. On the other hand, the reason for the appearance of the second peak can be understood from the response of

the effective permittivity of the nanocomposite material that has been investigated in Fig. 2**a**. At $\eta = 4 \times 10^{-4}$, the resonance peak is formed at 1179 nm; therefore this defect mode is formed due to the presence of the resonance peak at this wavelength.

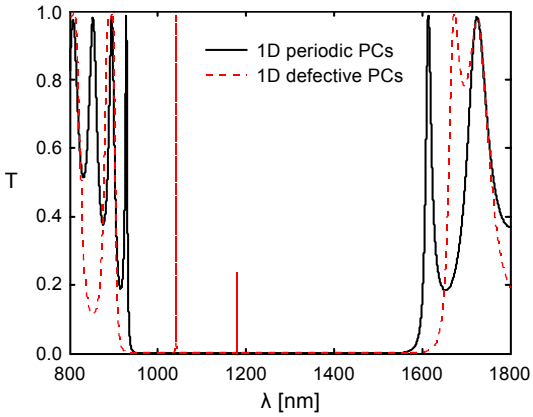

Fig. 3. The transmittance spectra for pure 1D PCs and 1D PCs with a nanocomposite defect at normal incidence.

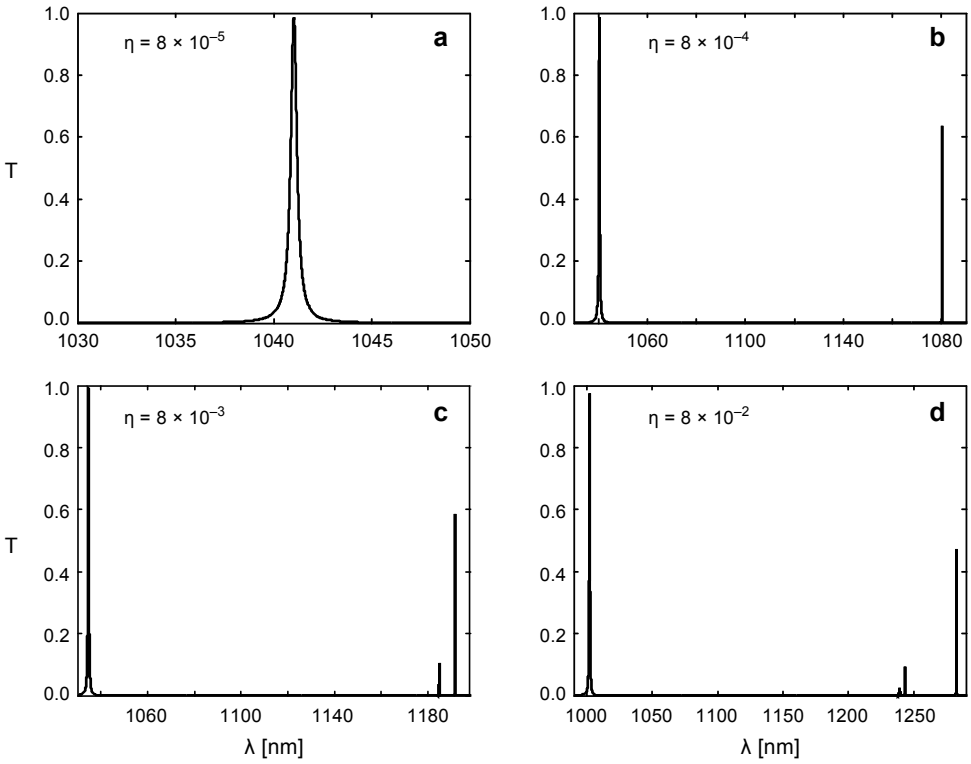

Fig. 4. The variation of transmittance with wavelength for 1D PCs with nanocomposite defect at different values of volume fraction: $\eta = 8 \times 10^{-5}$ (**a**), $\eta = 8 \times 10^{-4}$ (**b**), $\eta = 8 \times 10^{-3}$ (**c**), and $\eta = 8 \times 10^{-2}$ (**d**)

For more control on the properties of the defect modes that formed within the PBG, we investigate in Fig. 4 the effect of the volume fraction of the intensity of the defect peaks. For $\eta = 8 \times 10^{-5}$, a single defect peak is formed at 1041 nm with the intensity greater than 0.98 as shown in Fig. 4**a**. In addition, we observe the absence of the peak corresponding to the resonance peak of the effective permittivity due to the limited value of the resonance peak at this value of the volume fraction. For further increasing the value of the volume fraction to 8×10^{-4}, the position and the intensity of the defect mode formed due to the broken periodicity are almost unaffected. However, the defect mode corresponding to the resonance peak appeared at 1180 nm with the intensity of 0.637 as shown in Fig. 4**b**. As the volume fraction increases to 8×10^{-3} and 8×10^{-2}, the peak which appeared due to the broken periodicity is shifted to the lower wavelengths downwards. However, its intensity is almost unchanged as shown in Figs. 4**c** and 4**d**. Moreover, the defect mode of the resonance peak is shifted to the higher wavelengths upwards with the appearance of new defect modes.

Then, we demonstrate in Fig. 5 the effect of the operating temperature of the superconductor nanoparticles on the characteristics of the defect modes at $\eta = 4 \times 10^{-4}$. At $T = 1$ K, the first defect peak is observed at 1041 nm with the intensity higher than 0.98.

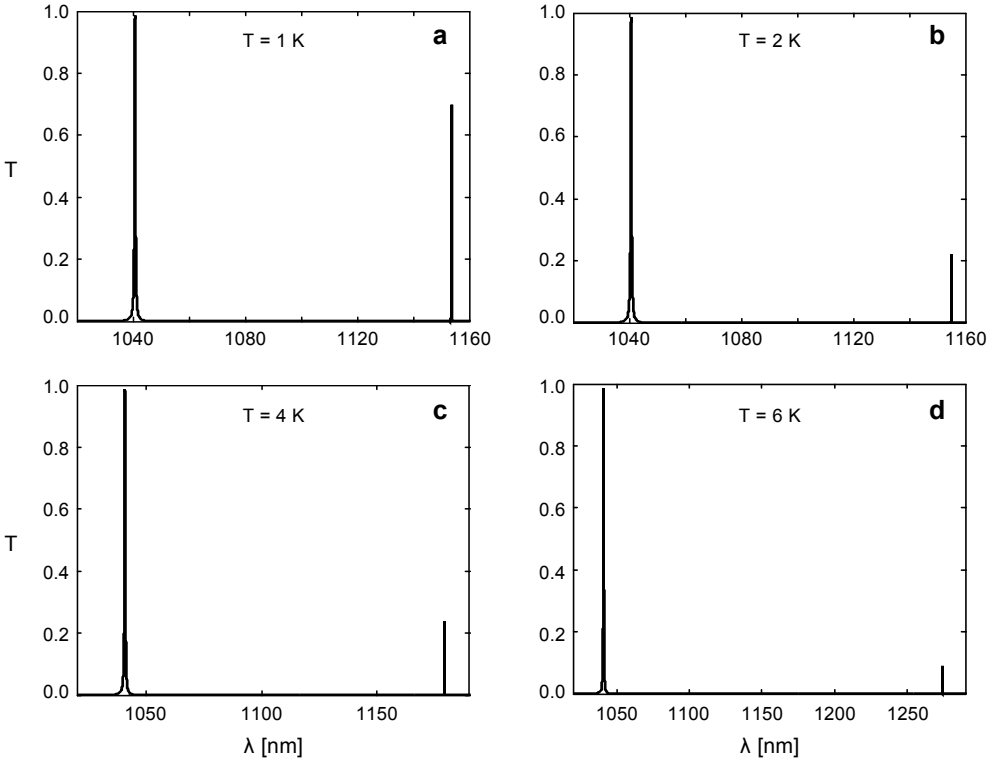

Fig. 5. The dependence of the position and the intensity of the defect modes on the operating temperature of the superconductor nanoparticles (see text for explanation).

Wherein, the second defect mode is formed at 1154 nm with the intensity equal to 0.7, as shown in Fig. 5**a**. As the operating temperature increased to 2 and 4 K, both the position and the intensity of the first defect mode are unchanged. Furthermore, the second defect peak is shifted from 1154 to 1155 nm and 1179 nm at $T = 2$ and 4 K, respectively, as shown in Figs. 5**b** and 5**c**. In addition, we observed a significant decrement within its intensity to reach 0.24. For further increase in the operating temperature to 6 K, the second peak is shifted upwards to a new wavelength with the decrement of its intensity due to the resonance peak shift towards higher wavelengths values with the increase of the operating temperature, as investigated in Fig. 2**b**.

Now, we discuss the effect of the permittivity of the dielectric material, in which the nanoparticles are arranged, on the intensity and the position of the defect peaks. For replacing MgF_2 of $\varepsilon_m = 1.92$ by Al_2O_3 of $\varepsilon_m = 3.77$, the defect peaks shifted towards the long wavelength regions. Also, the intensity of the first and the second peaks are decreased to 0.92 and 0.11, respectively, as shown in Fig. 6**b**. In the case of using Y_2O_3 with $\varepsilon_m = 3.22$, the two peaks shifted to 1087 and 1463 nm, respectively, with a slight decrease in the intensity of the first defect mode as shown in Fig. 6**c**. However, the intensity of the second defect mode begins to increase to reach 0.26. The second peak

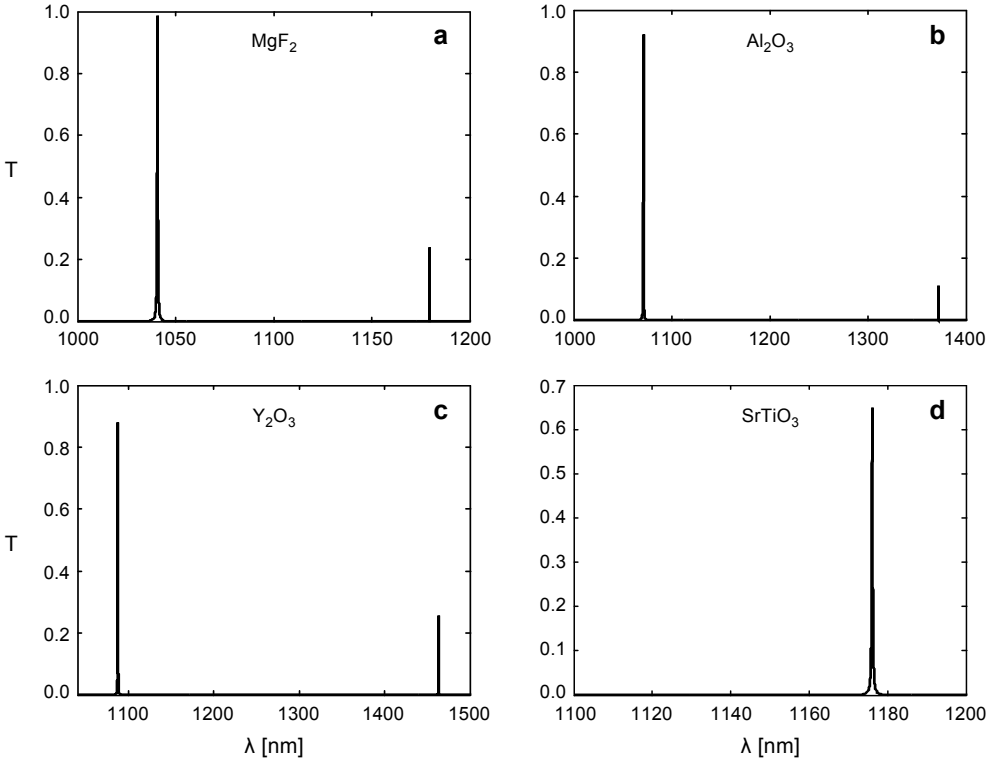

Fig. 6. The dependence of the intensity and the position of the defect modes on the permittivity of the host dielectric material (see text for explanation).

disappeared in the case of using $SrTiO_3$ with $\varepsilon_m = 5.94$. Moreover, the first defect mode is shifted to 1176 nm and its intensity decreased to 0.65, as shown in Fig. 6**d**. Therefore, the permittivity of the dielectric material plays an important role in controlling both the intensities and the positions of the defect modes.

Finally, we investigate in Fig. 7 the dependence of the defect modes properties on the threshold frequency of nanoparticles. For nanoparticles of Ga of $T_c = 1.09$ K and $\lambda_L = 120$ nm [32] in a dielectric material of MgF_2, Fig. 7**a** shows the appearance of only one defect mode localized at 1041 nm and having the intensity of more than 0.98. As Ga replaced Nb of $T_c = 9.2$ K and $\lambda_L = 85.7$ nm [31], there are two defect modes which are observed as shown in Fig. 7**b**. The first one is corresponding to the defect material and has the same position and the intensity in comparison with the case of Ga. Wherein, the second one is corresponding to the resonance peak and located at 1179 nm with the intensity of 0.23. For using V_3Si with $T_c = 17.1$ K and $\lambda_L = 70$ nm [32], the first defect mode is almost unaffected. Wherein, the second defect peak is shifted to 967 nm with the intensity of 0.69, as shown in Fig. 7**c**. Here, the position and the intensity of the second peak changed due to the change of the position and the value of the resonance peak with the threshold frequency. Finally, in the case of V ($T_c = 5.3$ K and $\lambda_L = 39.8$ nm) [32], the first peak is almost unaffected, wherein the second peak disappears as shown in Fig. 7**d**.

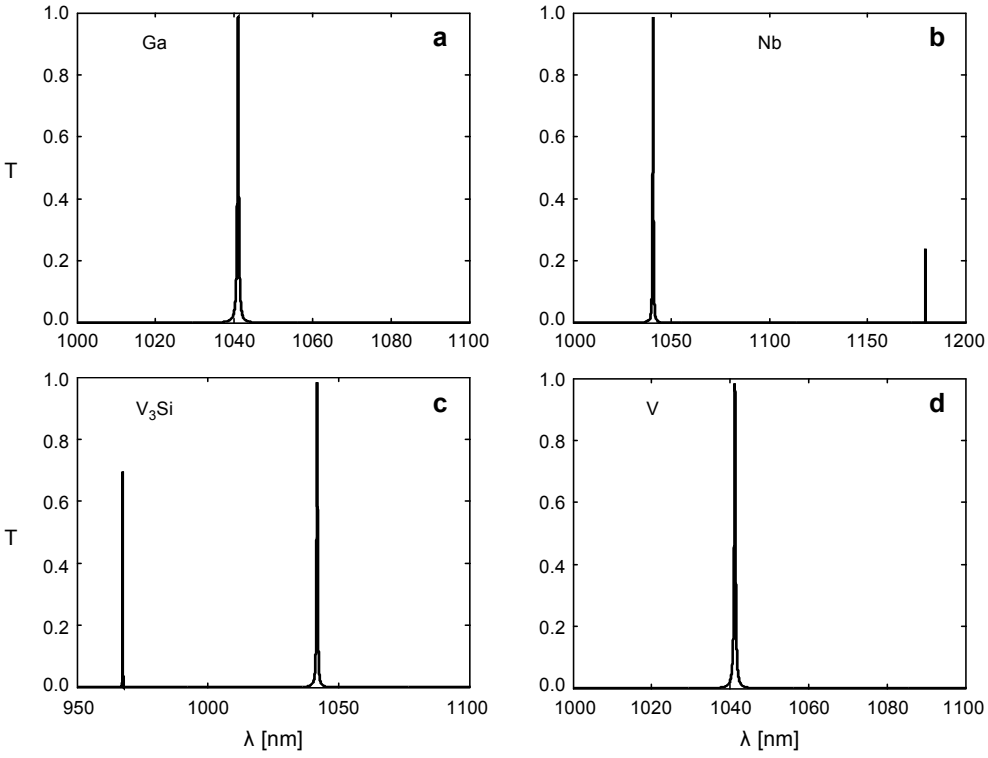

Fig. 7. The dependence of the intensity and the position of the defect modes on the threshold frequency of the nanoparticles (see text for explanation).

4. Conclusion

In summary, we investigate the transmittance characteristics of 1D PCs that contain a nanocomposite material as a defect. The numerical results indicate the significant dependence of the effective permittivity of the nanocomposite material on both the volume fraction and the operating temperature of the nanoparticles. Moreover, the inclusion of the defect layer leads to the appearance of two narrow defect peaks within the photonic band gap. Also, the intensity and the position of the defect peaks are controlled by changing the volume fraction, the operating temperature, the permittivity of the host material and the threshold frequency. Therefore, the proposed structure may be of potential use in many applications such as multichannel filters, laser and among optoelectronics applications. Moreover, the idea of nanocomposite material may be very promising when it is employed in different band gap materials such photonic crystals [33–35], what has not studied so far.

References

[1] Joannopoulos J.D., Johnson S.G., Winn J.N., Meade R.D., *Photonic Crystals: Molding the Flow of Light*, Princeton University Press, Princeton, NJ, USA, 2008.

[2] Elsayed H.A., El-Naggar S.A., Aly A.H., *Two dimensional tunable photonic crystals and n doped semiconductor materials*, Materials Chemistry and Physics 160, 2015, pp. 221–226.

[3] Fink Y., Winn J.N., Shanhui Fan, Chiping Chen, Michel J., Joannopoulos J.D., Thomas E.L., *A dielectric omnidirectional reflector*, Science 282(5394), 1998, pp. 1679–1682.

[4] Aly A.H., Elsayed H.A., El-Naggar S.A., *Tuning the flow of light in two-dimensional metallic photonic crystals based on Faraday effect*, Journal of Modern Optics 64(1), 2017, pp. 74–80.

[5] Aly A.H., Mohamed D., *BSCCO/$SrTiO_3$ one dimensional superconducting photonic crystal for many applications*, Journal of Superconductivity and Novel Magnetism 28(6), 2015, pp. 1699–1703.

[6] Yablonovitch E., *Inhibited spontaneous emission in solid-state physics and electronics*, Physical Review Letters 58(20), 1987, p. 2059.

[7] Yablonovitch E., *Photonic band-gap structures*, Journal of the Optical Society of America B 10(2), 1993, pp. 283–295.

[8] Aly A.H., Elsayed H.A., *Defect mode properties in a one-dimensional photonic crystal*, Physica B: Condensed Matter 407(1), 2012, pp. 120–125.

[9] Aly A.H., ElSayed H.A., *Tunability of defective one-dimensional photonic crystals based on Faraday effect*, Journal of Modern Optics 64(8), 2017, pp. 871–877.

[10] Aly A.H., Abdel Ghany S.E.S., Fadlallah M.M., Salman F.E., Kamal B.M., *Transmission and temperature sensing characteristics of a binary and ternary photonic band gap*, Journal of Nanoelectronics and Optoelectronics 10(1), 2015, pp. 9–14.

[11] Smith D.R., Dalichaouch R., Kroll N., Schultz S., McCall S.L., Platzman P.M., *Photonic band structure and defects in one and two dimensions*, Journal of the Optical Society of America B 10(2), 1993, pp. 314–321.

[12] Shi B., Jiang Z.M., Xun Wang, *Defective photonic crystals with greatly enhanced second-harmonic generation*, Optics Letters 26(15), 2001, pp. 1194–1196.

[13] Aly A.H., Aghajamali A., Elsayed H.A., Mobarak M., *Analysis of cutoff frequency in a one-dimensional superconductor-metamaterial photonic crystal*, Physica C: Superconductivity and its Applications 528, 2016, pp. 5–8.

[14] El-Naggar S.A., Elsayed H.A., Aly A.H., *Maximization of photonic bandgaps in two-dimensional superconductor photonic crystals*, Journal of Superconductivity and Novel Magnetism 27(7), 2014, pp. 1615–1621.

[15] ELSAYED H.A., EL-NAGGAR S.A., ALY A.H., *Thermal properties and two-dimensional photonic band gaps*, Journal of Modern Optics 61(5), 2014, pp. 385–389.
[16] KNIGHT J.C., BROENG J., BIRKS T.A., RUSSELL P.S.J., *Photonic band gap guidance in optical fibers*, Science 282(5393), 1998, pp. 1476–1478.
[17] ALY A.H., SABRA W., ELSAYED H.A., *Cutoff frequency in metamaterials photonic crystals within Terahertz frequencies*, International Journal of Modern Physics B 31(15), 2017, article ID 1750123.
[18] ALY A.H., ELSAYED H.A., HAMDY H.S., *The optical transmission characteristics in metallic photonic crystals*, Materials Chemistry and Physics 124(1), 2010, pp. 856–860.
[19] ALY A.H., SANG-WAN RYU, CHIEN-JANG WU, *Electromagnetic wave propagation characteristics in a one-dimensional metallic photonic crystal*, Journal of Nonlinear Optical Physics and Materials 17(3), 2008, pp. 255–264.
[20] ALY A.H., SANG-WAN RYU, HENG-TUNG HSU, CHIEN-JANG WU, *THz transmittance in one-dimensional superconducting nanomaterial-dielectric superlattice*, Materials Chemistry and Physics 113(1), 2009, pp. 382–384.
[21] ALY A.H., HENG-TUNG HSU, TZONG-JER YANG, CHIEN-JANG WU, CHANG KWON HWANGBO, *Extraordinary optical properties of a superconducting periodic multilayer in near-zero-permittivity operation range*, Journal of Applied Physics 105(8), 2009, article ID 083917.
[22] ALY A.H., EL-NAGGAR S.A., ELSAYED H.A., *Tunability of two dimensional n-doped semiconductor photonic crystals based on the Faraday effect*, Optics Express 23(11), 2015, pp. 15038–15046.
[23] ALY A.H., SABRA W., ELSAYED H.A., *Dielectric and superconducting photonic crystals*, Journal of Superconductivity and Novel Magnetism 26(3), 2013, pp. 553–560.
[24] VETROV S.YA., BIKBAEV R.G., TIMOFEEV I.V., *Optical Tamm states at the interface between a photonic crystal and a nanocomposite with resonance dispersion*, Journal of Experimental and Theoretical Physics 117(6), 2013, pp. 988–998.
[25] VETROV S.YA., AVDEEVA A.YU., TIMOFEEV I.V., *Spectral properties of a one-dimensional photonic crystal with a resonant defect nanocomposite layer*, Journal of Experimental and Theoretical Physics 113(5), 2011, pp. 755–761.
[26] LABBANI A., SAOUDI R., BENGHALIA A., *Photonic band gaps in one- and two-dimensional photonic crystals based on a nanocomposite of ZnS and glass*, Journal of Optics A: Pure and Applied Optics 11(8), 2009, article ID 085103.
[27] ORAEVSKII A.N., PROTSENKO I.E., *Optical properties of heterogeneous media*, Quantum Electronics 31(3), 2001, pp. 252–256.
[28] MOISEEV S.G., *Thin-film polarizer made of heterogeneous medium with uniformly oriented silver nanoparticles*, Applied Physics A: Materials Science and Processing 103(3), 2011, pp. 775–777.
[29] MOISEEV S.G., *Composite medium with silver nanoparticles as an anti-reflection optical coating*, Applied Physics A: Materials Science and Processing 103(3), 2011, pp. 619–622.
[30] BORN M., WOLF E., *Principles of Optics*, Cambridge, London, 1999.
[31] VAN DUZER T., TURNER C.W., *Principles of Superductive Devices and Circuits*, Edward Arnold, London, 1981.
[32] BUCKEL W., KLEINER R., *Superconductivity: Fundamentals and Applications*, VCH, Weinheim, 2004.
[33] ALY A.H., MEHANEY A., *Enhancement of phononic band gaps in ternary/binary structure*, Physica B: Condensed Matter 407(21), 2012, pp. 4262–4268.
[34] ALY A.H., MEHANEY A., EISSA M.F., *Ionizing particle detection based on phononic crystals*, Journal of Applied Physics 118(6), 2015, article ID 064502.
[35] ALY A.H., MEHANEY A., *Low band gap frequencies and multiplexing properties in 1D and 2D mass spring structures*, Chinese Physics B 25(11), 2016, article ID 114301.

Received December 15, 2016
in revised form March 29, 2017